Vibrational Coupling between Amide-I and Amide-A Modes Revealed by Femtosecond Two Color Infrared Spectroscopy[†]

Igor V. Rubtsov, Jianping Wang, and Robin M. Hochstrasser*

Department of Chemistry, University of Pennsylvania, Philadelphia, Pennsylvania 19104-6323

Received: August 21, 2002

Two color femtosecond infrared pump/probe spectroscopy has been used to study the vibrational dynamics and vibrational mode coupling of amide-A and amide-I/II modes within the same amide unit and those connected by a hydrogen bond for several model dipeptides: AcAla(H)OMe, AcAla(D)OMe, and AcProNHMe. Three spectral ranges were explored as follows: around 3 μm (amide-A(H) mode), 4 μm (amide-A(D) mode), and 6−8 μm (amide-I/II modes). The lifetime of the excited amide-A mode in nonhydrogen-bonded amide is found to be strongly dependent upon deuteration: 4.0 ps in AcAla(H)OMe and 0.58 ps in AcAla(D)OMe. The diagonal anharmonicities are found to be $\Delta_{N-D} = 110$ cm^{-1} and $\Delta_{N-H} = 144$ cm^{-1}, respectively, both much larger than the ca. 15 cm^{-1} for the amide-I mode. By pumping the amide-A band and probing the amide-I/II mode region, direct coupling between the amide-A and the amide-I/II modes has been observed. The off-diagonal anharmonicity between amide-A(D) and amide-I within the same amide unit has been measured to be 1.6 cm^{-1}, and this anharmonicity is larger (4.6 cm^{-1}) when a Fermi resonance component in the amide-I mode is involved. A mixed mode coupling with an apparent time-dependent off-diagonal anharmonicity is observed as a result of the relaxation of the amide-A mode to lower frequency modes, which are in turn coupled to the amide-I mode. This is found to be significant within the first half picosecond after the pump in the case of the deuterated AcAlaOMe since the T_1 of the amide-A(D) vibration in that example is short. The amide-A/amide-I coupling across the hydrogen bond in the self-hydrogen-bonded C$_7$ conformation of AcProNHMe is 1.4 cm^{-1}. The alignment of the transition dipoles (amide-I/II modes) relative to the known directions for N−H and N−D was measured and used to obtain structural information on the chemical structure of peptides. The direction of the amide-I transition moment in the molecular frame changes upon deuteration of the amide and upon hydrogen bonding of the N−H group of the amide. The angle between the amide-I transition moment and N−H in the same amide is determined to be 23 ± 3° for AcAla(H)OMe where the N−H group of the amide is weakly hydrogen-bonded in the C$_5$ conformation. This angle changes to 13 ± 4° for the deuterated compound and to 34.5 ± 3° when the N−H group is involved in strong intramolecular hydrogen bonding in the C$_7$ conformation (AcProNHMe). Two different conformers were observed for AcAla(H)OMe based on cross-peak anisotropy measurements. The structures of these conformers are assigned to C$_5$ (carbonyl) and C$_5$ (ester) conformations, where a five-membered ring is formed by the carbonyl or ester oxygen atom. A first principles simulation of the two color pump/probe signal based on the third order nonlinear polarization, assuming a homogeneous line width for the amide-I and amide-A modes, reproduces the data satisfactorily.

1. Introduction

Two-dimensional infrared (2D IR) spectroscopy has recently been proposed as a means to determine the structural dynamics of biological assemblies having amide-I modes.[1−9] In 2D IR, sequences of femtosecond infrared pulses are used to manipulate vibrational coherences leading to knowledge of angular distributions of the amide groups and their intermode anharmonicities. These anharmonicities are related to the couplings between amide units and hence to their spatial arrangements. The same 2D IR experiment measures the dynamics of the distributions of amide-I vibrational frequencies, which are related to the distributions of structures that occur in equilibrium. Although 2D IR has great promise for biological applications,[10−12] a number of fundamental issues regarding the dynamical responses

of molecular vibrations in solutions first need to be addressed quantitatively. In addition, models for the potential energy surfaces of peptides suitable for generating mode coupling mechanisms need to be more fully explored.

A significant improvement in the utility of 2D IR could be expected if the infrared pulse sequence was chosen to manipulate two or more different types of molecular vibrations. This experiment could be done by constructing the sequences from infrared sources having different frequencies. Such two color experiments may yield intermode couplings and provide additional structural constraints. A variety of two color pulse sequences for 2D IR experiments were recently proposed along with discussion of their response functions.[13−15] Besides, the amide-I mode, which is mainly the C=O stretch, the N−H stretch, or the amide-A mode, is also a useful indicator of secondary structure.[16−20] Therefore, a two color 2D IR experiment involving the amide-I modes at 6 μm and the amide-A modes at 3 μm is expected to provide useful new information

Vibrational Coupling between Amide-I and Amide-A Modes

J. Phys. Chem. A, Vol. 107, No. 18, 2003 **3385**

on peptide structure and dynamics. However, nothing is known experimentally about the coupling of amide-I and -A modes, even when they are on the same amide unit. This coupling must be known in order to develop reliable models for the coupling of different amide units. For example, for a dipeptide with two amide units (1 and 2), there are four states in the amide-I/amide-A combination band region: $I_1 + A_1$, $I_1 + A_2$, $I_2 + A_1$, and $I_2 + A_2$. A structurally based model for the relative energies of these states requires knowledge of the I_n and A_n coupling ($n = 1, 2$). The through bond part of the coupling is expected to be small because the N—H mode is highly localized and involves mainly hydrogen motions. Nevertheless, the interamide couplings that depend on secondary structure, perhaps through transition charge interactions,[1,21] will be important. Therefore, it is important to have experimental measures, in solutions, of the mixed mode anharmonic coupling within a single amide unit and amide units separated by across hydrogen bonds.

Determining the relative orientations of bonds in an individual peptide group is important in understanding higher order structural elements of proteins and peptides. However, determination of the angular relationships among key functional groups in small peptides is still a challenging task. One way to obtain such information is through the determination of the transition dipole moment directions of vibrational modes. However, even for a simple single amide unit, the direction of the various transition dipole moments can be molecular structure-dependent, and large discrepancies are found between experimental measurements and theoretical calculations. For instance, the dipole moment derivative of the amide-I mode was found experimentally between +15 and +25° from the C=O bond direction in a model compound *N*-methylacetamide (NMA),[22] whereas the results obtained from ab initio calculations range from −19 to +20° in NMA or for different model compounds, depending on the selection of the force field.[21,23−27] For the amide-A mode, the direction of the transition moment relative to the C=O bond was determined to be either +8 or +28° in NMA,[22] whereas it is +13° in acetanilide.[28] The present approach provides an effective way to determine the average angles between different transition moments for peptides in solutions.

The third order 2D IR experiment can be carried out by heterodyning the radiated infrared field with either the probing pulse itself [29,30] or a fourth infrared pulse.[2,6] The former is a pump/probe technique in which an infrared pulse with a narrow frequency bandwidth excites the sample and a shorter, broad band pulse probes it before it is frequency-dispersed. The ultrafast infrared pump/probe technique has proved to be an effective way of examining intra- and intermolecular vibrational relaxation in a wide variety of examples that include solutions,[15,31−37] neat liquids,[38−40] surfaces,[41−44] and numerous theoretical descriptions of the expected IR/IR pump/probe signals that have been developed.[13,45−47] Two color infrared pump/probe methods requiring the generation of two separate infrared frequencies were previously used in studies of surfaces,[41] liquid water,[14] alcohols,[15,48] carbonmonoxy myoglobin and hemoglobin,[49] and aqueous molecular ions.[33]

In this work, we present IR pump/probe measurements of the coupling and angular relations of the amide-A, amide-I, and amide-II modes in single amide units and between units connected by a hydrogen bond. To extract the structural parameters from the pump/probe measurements, it was necessary to characterize as fully as possible the underlying vibrational dynamics.

2. Material and Methods

2.1. Two Color Midinfrared Pump/Probe Setup. A two color midinfrared pump/probe transient spectrometer was constructed. It was based on a Ti-sapphire laser system (Clark-MXR CPA2001) with a fiber oscillator and a regenerative amplifier, operating at 775 nm (pulse duration, 130 fs; repetition rate, 1 kHz; and pulse energy, 700 μJ). The output of the regenerative amplifier was split into two parts to pump two IR OPAs, each producing ca. 60 μJ/pulse total energy in signal and idler beams. Two separate difference frequency generators (DFG) produced mid-IR beams tunable from 3 to 10 μm (at 6 μm: bandwidth ca. 120 cm^{-1}, pulse duration ca. 150 fs, pulse energy ca. 0.7 μJ/pulse). The output of one DFG unit was used as a pump and tuned to generate either a 3 or a 4 μm beam that could be centered at the amide-A band (N—H or N—D stretching mode). A narrow band IR filter (Optical Coating Laboratory Inc., CA) was used to further confine the bandwidth of the 4 μm pump beam to 37 cm^{-1} (full width at half-maximum (fwhm)), which corresponded to a pulse duration of 390 fs and overall instrument response time of 440 fs. A broadband excitation (fwhm 100 cm^{-1}) was used in the 3 μm region yielding an instrument response time of ca. 200 fs. Another DFG unit was used to generate probe and reference pulses (bandwidth ca. 160 cm^{-1}; pulse duration, 140 fs; pulse energy ca. 0.05 μJ/pulse), which were tunable across the range from 1300 to 3550 cm^{-1}. Polarization of the pulses was controlled by a set of wire-grid polarizers. The time zero was determined by monitoring the cross-phase modulation in the solvent.

2.2. Materials and Sample Preparation. The model peptides used in this work, acetyl-alanine-OMe (AcAlaOMe) and acetyl-proline-NHMe (AcProNHMe), were purchased from Bachem Co. The deuteration of the AcAlaOMe compound was achieved by dissolving it in D$_2$O and lyophilizing it overnight, providing a deuteration of 96% of the amides. The deuterated sample was dissolved in CDCl$_3$ whereas the nondeuterated ones were dissolved in CHCl$_3$, both at a concentration of ca. 20 mM. Samples were held in a rotating CaF$_2$ cell with a path length of 510 μm. The AcProNHMe sample was prepared in CHCl$_3$ at a concentration of 120 mM with a path length of 100 μm. All of the measurements were performed at room temperature (22 ± 1 °C).

2.3. Fitting and Simulation Methods. The transient signal for a single oscillator was a sum of a transient absorption ($v = 1 \rightarrow v = 2$), ground state bleach (decrease in 0→1), and stimulated emission (1→0). The frequency of the 1→2 transition was anharmonically shifted from the 0→1 transition, and its extinction coefficient was approximately twice as large as that of 0→1. The anharmonic shift determined the strength and shape of the transient spectrum, which we refer to as the diagonal signal. When combination bands were accessed, the off-diagonal anharmonicity caused the appearance of a similarly shaped signal, which we refer to as the cross-peak or off-diagonal signal: of course, when there was no coupling between the modes and all of the relevant transitions had the same width, there was no such difference signal. Because of the finite line widths, which can differ for 0−1 and 1−2 and combination band transitions, and the effects of hole burning, which are determined by the excitation pulse spectrum and the inhomogeneous distribution, the observed peak separations did not yield the anharmonicities directly. An exception occured for the case of N−H and N−D modes where the diagonal anharmonicity was sufficiently large that it was essentially equal to the splitting between the bleach and the new absorption. However, for the combination bands, which generally exhibited anharmonic shifts
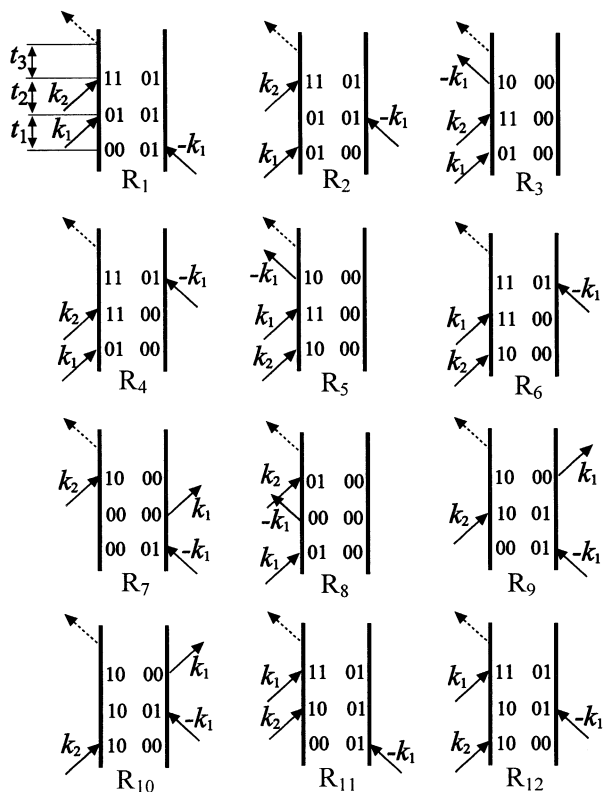
Figure 1. Liouville pathways that are involved in the pump/probe experiment. Response functions from those diagrams are used to simulate the experimental data.
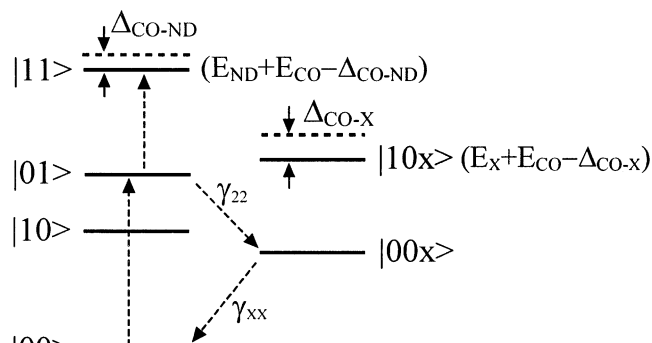

Figure 2. Three level model to describe the origin of the mixed mode coupling in the observed pump/probe off-diagonal cross-peak signal. It is assumed that the N−D relaxes to the unknown state "x" with the rate constant of $1/T_{1,ND}$. This state is coupled with amide-I and relaxes to the ground state with the rate constant of $1/T_{1,x}$. This model is applied to both components in the amide-I mode in the case of the N−D excitation.

that were smaller than the line widths, the underlying parameters were only obtained by globally fitting the difference spectra obtained for different times. The fitting of the spectra required knowledge of the relative values of the peak extinction coefficients and sufficiently accurate representations of the spectral line shapes obtained from FTIR measurements. In the present cases, Lorenzian representations of these line shapes were found to be adequate. Because the amide-I and -A bands were not symmetric or did not exhibit shoulders, the contributions of all of the contributing bands were required to fit the data. One approach would be to just fit the kinetic spectra to a number of components; another would be to curve fit the FTIR to obtain its underlying components, which could then be used to fit the kinetic spectra. We combined both of these approaches by simultaneously fitting both FTIR and transient spectra. The component bands from the combined fits are shown in some of the figures. All fitting results incorporated convolution with the instrument response function.

The two color pump/probe signals were also simulated from the third order nonlinear polarization[13] using the measured dynamical and frequency parameters. The relevant Liouville pathways are shown in Figure 1. The response functions were similar to those reported previously.[1,13] In Figure 1, the density operator indices correspond to the ground state, $|00\rangle$, the amide-I state excitations, $|10\rangle$ and $|20\rangle$, the amide-A state excitations, $|01\rangle$ and $|02\rangle$, and the amide-I/amide-A combination band, $|11\rangle$.

Population flow into modes other than those amide modes that are excited (IVR) is modeled by allowing the population of the N−H mode to relax into a fifth level (labeled x in Figure 2) whose anharmonic coupling to amide-I can be parametrized. The deexcitation of x is assumed to repopulate the ground state. The presence of the state x provides a model for the situation in which the apparent N−H/amide-I anharmonicity is time-dependent. The state x may represent the effect of many states

of the system. Its anharmonicity, which is a parameter found by fitting experimental data to the model of Figure 2 at a given delay time, is a population-weighted average of the off-diagonal anharmonicities of these many states and the amide-A mode. When the amide-A mode (N−D or N−H) is pumped, there will be an immediate change in the amide-I mode spectrum if there is a finite coupling between the modes. We know from previous experiments that the intensities for amide-I mode excitations obey harmonic rules[1] to adequate experimental accuracy, in which case when the lifetime of the pumped state is much longer than the pulse width, the off-diagonal anharmonicities and the line width of the induced transition from the amide-A state to the combination band are the remaining variables in the fitting procedure. Otherwise, the model of Figure 2 must be fitted to the kinetic and spectral data. In fact, we find significant changes with time of the amplitudes and peak separations of the signals for the N−D mode excitation and amide-I probing. However, the time resolution of the experiment is shorter than the population relaxation time of amide-A and so a meaningful extrapolation to zero time delay is possible.

In the spectral region of the N−H stretch mode, the linear spectrum of the solvent (chloroform) has broad, weak absorption, which can be excited by the pump pulses. The transient signals in this spectral region from the solvent only constitute up to ∼20% of the signals obtained from the peptides. The time evolution of this solvent transient contains fast (∼300 fs) and slow (several picoseconds) components. However, this signal is quite reproducible and can be subtracted from the peptide response. All of the relaxation measurements reported here showed this small fast kinetic component, which was subtracted off to obtain the quoted experimental relaxation times.

The overall response functions were calculated including all of the diagrams of Figure 1 yielding the total pump/probe signal as a function of the delay times and the shapes of the pump and probe pulses. Calculations were performed by using the MATLAB platform (The Math Works Inc.) on a Pentium III computer. The time scale was from −1.5 to 9.5 ps in steps of 9 fs.

3. Results

The linear IR spectra are described in Section 3.1, the kinetics and transient spectra are described in Section 3.2, and the anisotropy results are described in Section 3.3. Summaries of the main results are displayed in Table 1.
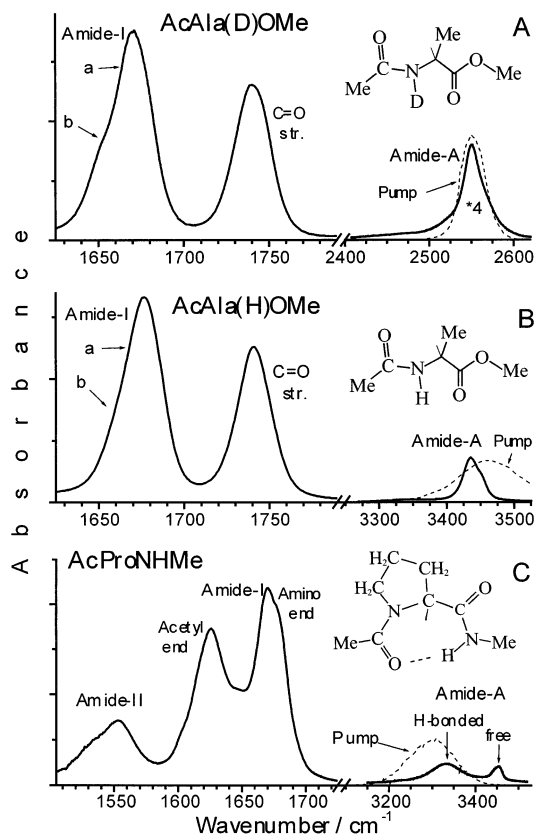
Vibrational Coupling between Amide-I and Amide-A Modes

J. Phys. Chem. A, Vol. 107, No. 18, 2003 **3387**

Figure 3. Linear infrared absorption spectrum of AcAla(D)OMe (A), AcAla(H)OMe (B), and AcProNHMe (C) in chloroform in the selected regions. The spectra of the respective pump pulses and the sketches of the chemical formulas are shown.

3.1. Linear IR Spectra. The relevant parts of the FTIR spectra of AcAlaOMe, AcAla(D)OMe, and AcProNHMe in chloroform are shown in Figure 3. The spectra of the three different pump pulses used for excitation of the amide-A modes are also shown in Figure 3. For AcAlaOMe, the acetyl C=O forms the amide grouping along with the Ala N−H, yielding an amide-I band in the 1645−1680 cm^{-1} region. A red shift of 4−5 cm^{-1} is found upon N−H/N−D exchange. The methyl ester carbonyl band at higher frequency, ∼1740 cm^{-1}, is not affected by N−H deuteration. The amide-I band of AcAla(D)-OMe has evident overlapping components. The weaker *b* component, on the low-frequency side, is slightly narrower (18 cm^{-1}, fwhm) than the stronger *a* component (22 cm^{-1}, fwhm). The relative intensity of these two components is 1:0.22. This ratio was determined to be independent of concentration in the range 0.2 μM to 20 mM in CDCl$_3$, supporting the notion that these bands do not arise from aggregates of the peptide. Therefore, the *b* component is either a minority conformation of the peptide or a Fermi resonance due to a nearby combination band. In AcAla(H)OMe, the amide-I band also exhibits two components but they have a smaller splitting than that in the deuterated compound, where their presence is evidenced only as an asymmetry of the band in the FTIR spectrum (Figure 3B). Further analysis reveals that Fermi resonance is the most probable origin of the amide-I band substructure in both isotopomers.

The N−D mode band at 2550 cm^{-1} (Figure 3A) has an overall spectral width of ca. 35 cm^{-1} (fwhm), with an integrated area of 13% of the amide-I band. There is a clear shoulder on the high-frequency side of the band. The N−H band at ca. 3436 cm^{-1} in AcAla(H)OMe (Figure 3B) has an integrated area of 25% of the amide-I band. It shows clearer substructure than

AcAla(D)OMe with a weaker and narrower component at 3450.3 cm^{-1} (fwhm = 16 cm^{-1}) and a stronger component at 3435 cm^{-1} (fwhm = 25 cm^{-1}), with the area ratio of 1:5. The former is in the frequency range for free N−H absorption, while the latter is in the range found for weakly hydrogen-bonded structures. The splitting of the amide-A band, as will be shown below, probably originates from populations of different secondary structures in both isotopomers. At higher concentration, the spectrum of the N−H region changes due to aggregation evidenced by appearance of more red-shifted N−H absorption bands at ca. 3300 cm^{-1}. The concentration dependence shows that the bands at 3435 and 3450.3 cm^{-1} belong to isolated (nonaggregated) peptides.

The AcProNHMe dipeptide allows us to investigate the effect of intramolecular hydrogen bonding on the coupling between amide-A and amide-I modes in the same amide unit. The coupling between the amide-A and amide-I modes on either side of the intramolecular hydrogen bond has also been studied for AcProNHMe. It is known that in nonhydrogen-bonding solvents AcProNHMe adopts the C$_7$ self-H-bonding conformation,[11,36,50] thus presenting a model for the γ-turn motif. The FTIR absorption spectrum of this compound in the amide-A band region consists of two bands: a small sharp peak at 3452 cm^{-1} (fwhm = 27 cm^{-1}) caused by nonhydrogen-bonded amides and a strong and broad band at 3333 cm^{-1} (fwhm = 119 cm^{-1}) originating from the C$_7$ self-hydrogen-bonded conformation,[18,51] with an area ratio of 1:5.8. In the experiment reported here, the pump frequency was tuned to excite predominantly the peptides in the C$_7$ conformation, as shown in Figure 3C.

The two amide-I bands of AcProNHMe, a lower frequency band at 1625 cm^{-1} (acetyl end) and one at 1670 cm^{-1} (methylamino end), exhibit a substructure. The amide-I (methylamino end) band is narrower and can be uniquely deconvoluted into two bands at 1680 (fwhm 17 cm^{-1}) and 1668.8 cm^{-1} (fwhm 20 cm^{-1}) with the area ratio of 1:2. The amide-I (acetyl end) band is broader and asymmetric. Spectral deconvolution, supported by transient data, gives two components at 1626.5 (fwhm 30 cm^{-1}) and 1619 cm^{-1} (fwhm 27 cm^{-1}) with the area ratio of 3.8:1. The amide-II (methylamino end) band is observed at 1550 cm^{-1} and consists of two clear subbands: at 1554 (fwhm 26 cm^{-1}) and 1534 cm^{-1} (fwhm 34 cm^{-1}).

3.2. Pump/Probe Spectra and Kinetics. We now present the data on diagonal and cross-peak regions for each of the peptides, including the results of fitting spectra and kinetics leading to the diagonal and off-diagonal anharmonicity parameters and lifetimes of the various states. The results for AcAla-(D)OMe are presented in most detail since they illustrate the typical approach used in all examples.

3.2.1. Amide-A Excitation in AcAla(D)OMe. Diagonal Region. Figure 4A shows the pump/probe transient spectrum of the N−D mode of AcAla(D)OMe at a short delay time (∼150 fs). The bleach (decrease of |00⟩→|01⟩ due to removal of population from |00⟩ and stimulated emission bands (|01⟩→|00⟩)) is observed at ca. 2550 cm^{-1} (full width of ∼35 cm^{-1}), and the new absorption (|01⟩→|02⟩) is observed at ca. 2440 cm^{-1} (fwhm ∼156 cm^{-1}) with the diagonal anharmonicity of 110 cm^{-1}. The decay of the transient absorption at 2450 cm^{-1} is single exponential with the decay time of 610 ± 60 fs (Figure 4B). At the bleach region (2550 cm^{-1}), the fit yielded 570 ± 40 fs and an additional slow component of 5.5 ± 0.8 ps (9%). A full analysis of the time evolution of the transient spectra (data not shown) ensures that the fast component (average value, 580 fs) is the population relaxation time of the amide-A(D) mode. The
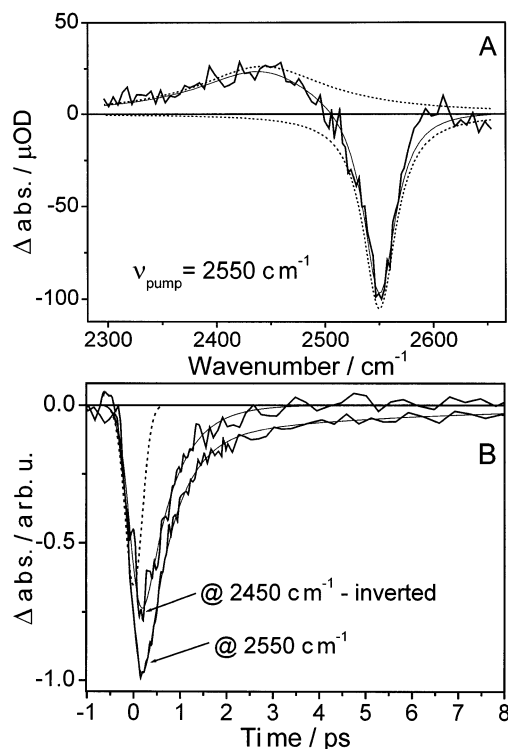
Figure 4. (A) Pump/probe transient spectrum of the N−D stretching mode of AcAla(D)OMe in the amide-A region measured at a 150 fs delay. The dotted lines show the fit to bleach and new absorption signals. (B) Kinetics at 2550 and 2450 cm^{-1} measured at magic angle polarization. The decay at 2450 cm^{-1} is inverted for comparison. The instrument response function is shown as a dotted line. Best fits of exponentials are shown as thin solid lines.
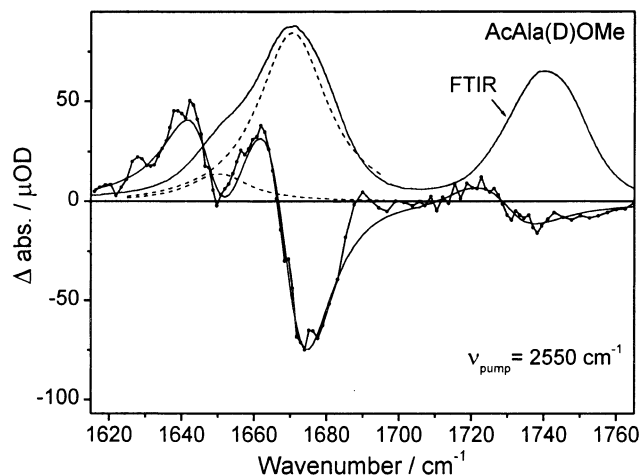

Figure 5. Off-diagonal transient spectra in the amide-I/C=O stretch region of AcAla(D)OMe at a time delay of 150 fs along with the FTIR spectrum. The best fit (using transients and linear FTIR) is shown by a thin solid line. Dotted lines show the spectral components of the amide-I band obtained by the fit.

slow component is assigned to another relaxation process and is discussed in Section 4.5.

Cross-Peak Region. Figure 5 shows the pump/probe off-diagonal signal in the 6 μm region. Linear IR spectra are also shown in Figure 5 for comparison. All of the observed transient spectral features are in accordance with expectations from the corresponding linear IR spectra. By pumping the N−D band at 2550 cm^{-1} (Figure 5), instantaneous responses at the amide-I frequencies are observed, indicating a direct mode-coupling between these modes and amide-A. However, the N−D
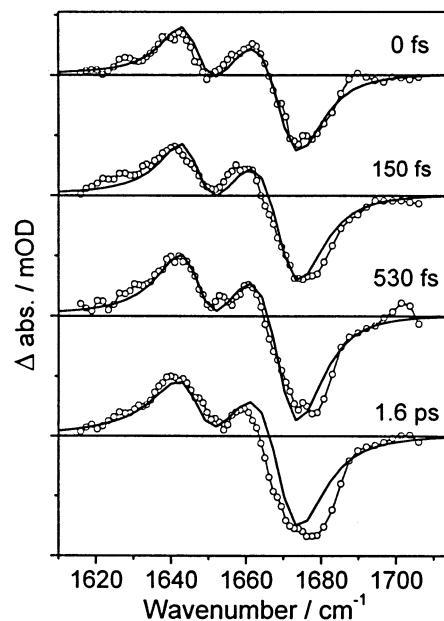

Figure 6. Off-diagonal pump/probe spectra in the amide-I region of AcAla(D)OMe acquired at different time delays: 0 fs, 150 fs, 530 fs, and 1.6 ps. The simulated transient spectra are shown as thick solid lines (see text for details). The following are the modeling parameters. (i) Amide-A data: 2550 cm^{-1}, Δ_{AA} = 110 cm^{-1}, T_1 = 0.58 ps, T_2 ($|00\rangle{\rightarrow}|01\rangle$) = 0.26 ps; (ii) amide-A/amide-Ia combination: 1671 cm^{-1}, Δ_{AIa} = 1.6 cm^{-1}, T_2 ($|0_a1\rangle{\rightarrow}|1_a1\rangle$) = 0.41 ps; amide-Ia: T_1 = 1.17 ps, T_2 ($|0_a0\rangle{\rightarrow}|1_a0\rangle$) = 0.40 ps; (iii) amide-A/amide-Ib combination: 1651 cm^{-1}, Δ_{AIb} = 4.6 cm^{-1}, T_2 ($|0_b1\rangle{\rightarrow}|1_b1\rangle$) = 0.55 ps; amide-Ib: T_1 = 1.17 ps, T_2 ($|0_b0\rangle{\rightarrow}|1_b0\rangle$) = 0.48 ps; (iv) amide-Ia/x combination: Δ_{xIa} = 4 cm^{-1}; T_2 ($|0_a0x\rangle{\rightarrow}|1_a0x\rangle$) = 0.38 ps; (v) amide-Ib/x combination: Δ_{xIb} = 7 cm^{-1}; T_2 ($|0_b0x\rangle{\rightarrow}|1_b0x\rangle$) = 0.54 ps.

relaxation time is sufficiently short that at zero delay time the optically pumped mode is not the only populated mode.

One negative feature at 1673 cm^{-1} and two positive features at 1643 cm^{-1} and 1662 cm^{-1} are found. This transient spectrum indicates that the signal is composed of two pairs of bleach and absorption signals, corresponding to the two components (*a* and *b*) observed in the amide-I mode linear spectra (Figure 3A). The transient peaks on the low- and high-frequency sides (1640 and 1673 cm^{-1}) are most clearly separated from the others. A spectral deconvolution yields two bleach signals at 1652 and 1671 cm^{-1} and two new absorptions at 1640 and 1650 cm^{-1}. The observation of the off-diagonal signals at the higher frequency Ala carbonyl region (1740 cm^{-1}) indicates that there is an anharmonic coupling between the free amide-A and the C=O stretch mode at the ester end.

Figure 6 shows the cross-peak signals at various delay times in the amide I region after pumping the N−D band at 2550 cm^{-1}. The coupling between N−D and amide-I appears to change with delay time. Two positive bands and one negative signal are always seen in the region of 1620−1700 cm^{-1} as the delay time changes from 0 to 1.6 ps, indicating that two pairs of bleach and absorption signals are always involved. These are the signals related with the components *a* and *b* of the amide-I mode as indicated above. However, their relative intensities (and peak positions) change as a function of time, as if the anharmonicity was time-dependent. The persistence of the off-diagonal cross-peak signal even when the N−D population is completely relaxed proves that the shifts are caused by coupling of the amide-I to other modes besides N−D. The off-diagonal anharmonicities obtained from the analysis of these spectra and kinetics are listed in Table 1. They are smaller than the spectral line widths of the amide-I or carbonyl transitions.

TABLE 1: Experimental Relaxation and Angular and Coupling Data for AcAla(D)OMe, AcAla(H)OMe, and AcProNHMe[a]

dipeptide	T_1 (ps)	Δ_{AA} (cm^{-1})	Δ_{AI} (cm^{-1})	$\langle\cos^2\xi_{AI}\rangle$	θ_{AI} (°)
		In the Same Amide			
AcAla(D)OMe	0.58 ± 0.04 (91%)	110 ± 7	1.6 ± 0.4[b]	0.94 ± 0.05	13 ± 4
	5.5 ± 0.8 (9%)		4.6 ± 0.7[c]		
AcAla(H)OMe	4.0 ± 0.4	144 ± 7	1.4 ± 0.4[b]	0.88 ± 0.05	23 ± 3
			2.6 ± 0.8[c]		
AcProNHMe (C$_7$)	0.58 ± 0.05[d]	165 ± 15	3.5 ± 0.3	0.67 ± 0.05	34.5 ± 3
			3.5 ± 0.3		
		Between N and C Terminal Ends			
AcAla(D)OMe			0.45 ± 0.2[e]		
AcAla(H)OMe		C$_5$(carbonyl)	1.8–3	1–0.67	0–35
		C$_5$ (ester)	0.3–1	0–0.22	62–90
		Free N−H[f]	0.2–1.2		
AcProNHMe (C$_7$)			1.4 ± 0.4	0.19 ± 0.05	64 ± 4
			5.5 ± 1		

[a] Amide-A mode lifetime (T_1), diagonal (Δ_{AA}), and off-diagonal (Δ_{AI}) anharmonicities and angles (θ_{AI}) between amide-A (NH or ND) and amide-I transition dipoles. [b] For amide-Ia band. [c] For amide-Ib band. [d] The lifetime for the hydrogen bonded N−H. [e] Averaged across the band (the value for the H isotope is 1.2 cm^{-1}). [f] Conformation with nonhydrogen-bonded N−H.
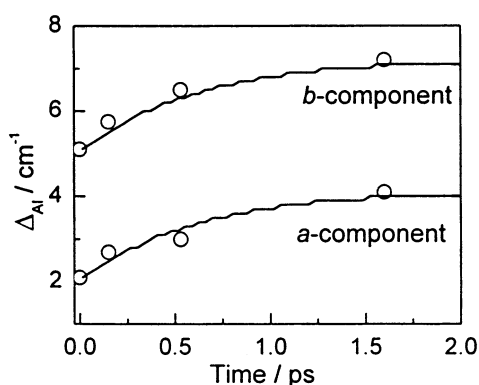
Figure 7. Apparent off-diagonal anharmonicity for two components (*a* and *b*) in AcAla(D)OMe as a function of delay time.
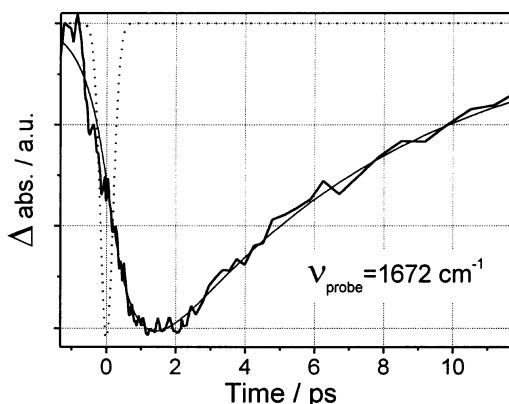
Figure 8. Cross-peak dynamics measured at 1672 cm^{-1} in AcAla-(D)OMe with N−D excitation. The signal from solvent measured at the same wavelength and contributing at zero time delay was subtracted. The fit to two exponentials is shown as a thin solid line. $\tau_{rise} = 670 \pm 50$ fs, $\tau_{decay} = 7.0 \pm 0.8$ ps, and $T_2 = 0.49$ ps. The instrument function is also shown.

For the N−D peptide, Figure 7 shows the apparent off-diagonal anharmonicities as a function of delay time. Each point is obtained by fitting the time-dependent spectra in the manner described in Section 2.3: we assume that a population-weighted distribution of anharmonically shifted modes is being observed. The off-diagonal anharmonicity for the amide-I components *a* and *b* at zero delay time is 2.1 ± 0.5 and 5 ± 1 cm^{-1}, respectively. At 1.6 ps delay time, these two apparent anharmonicities become 4 ± 0.5 and 7 ± 1.5 cm^{-1}. The solid line in Figure 7 is a simulation that will be described later.

Figure 8 shows the cross-peak kinetics measured at 1672 cm^{-1}. The kinetic signal shows finite growth time of the signal, evidenced in Figure 8 by the peak in the kinetic trace occurring at the delay times in excess of 1 ps. There is clearly a time evolution of the effective anharmonic shift. At times beyond 1 ps, the N−D population is greatly diminished ($T_1 = 580$ fs) so the amide-I transitions seen in the transients must originate in levels that were reached by the N−D relaxation. These modes (or mode) display an overall relaxation time of 7.0 ± 0.8 ps. By global analysis of the spectral and kinetic data in terms of these populations, we find an apparent time-dependent anharmonicity, presumably because these levels to which N−D relaxes couple more strongly to the amide-I mode than does the N−D mode. The decay time of 7 ps represents an average time for the cooling process; it is comparable to the time of 10 ps obtained recently for AcProNH$_2$ in methylene chloride after amide-I band excitation.[36] The off-diagonal anharmonicities for amide-A and amide-Ia/-Ib of the same amide unit are found to be, respectively, 1.6 ± 0.4 and 4.6 ± 0.7 cm^{-1} from this analysis. The averaged coupling of the amide-A mode and the ester carbonyl (1740 cm^{-1}) determined from the magic angle (Figure 5) is much smaller, at 0.45 ± 0.2 cm^{-1}.

3.2.2. Amide-A Excitation in AcAla(H)OMe. Diagonal Peak Region. Figure 9A shows the spectrum of AcAlaOMe obtained for the N−H band excitation at 350 fs time delay. By using low concentration of the sample and tuning the pump to the high-frequency side of the amide-A band, it was possible to ensure that 95% of the excited population corresponded to the isolated peptides. The bleach and stimulated emission contribute to the spectrum at 3436 cm^{-1}, and the new absorption ($|01\rangle > \rightarrow |02\rangle$) is at 3292 cm^{-1}. As the pump spectrum is broader than the whole N−H absorption band of the isolated peptides, both subbands at 3435 and 3450.3 cm^{-1} are excited. While the diagonal anharmonicity of the main component at 3435 cm^{-1} can be accurately determined, the diagonal anharmonicity for the minor component (3450.3 cm^{-1}) is less certain and is assumed to be the same as that for the major component. A diagonal anharmonicity of 144 ± 7 cm^{-1} is obtained, which is significantly larger than that found for the amide-A(D) mode. The spectral width of 43 cm^{-1} for the transient absorption ($|01\rangle \rightarrow |02\rangle$) at ~3292 cm^{-1} is about twice the ground state absorption width of 25 cm^{-1} for the main component (see Figure 3B). However, it is considerably less than the 156 cm^{-1} width found for the transient absorption band of the amide-A(D) mode (Figure 4A).
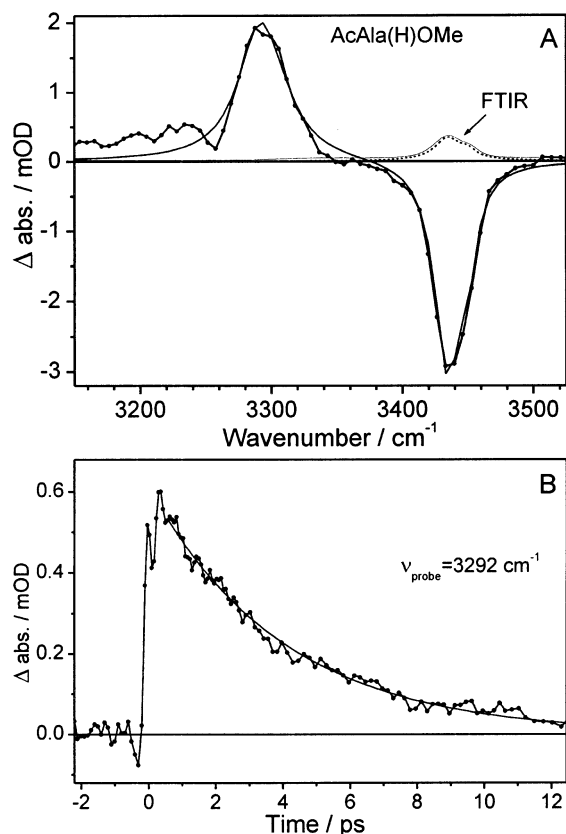
Figure 9. (A) Diagonal transient spectrum of the amide-A mode of AcAla(H)OMe measured at 350 fs time delay along with the linear absorption spectrum (FTIR). The fit of both spectra is shown as a thin solid line for transient spectrum and dotted line for FTIR spectrum. (B) Decay dynamics measured at 3292 cm^{-1} with magic angle polarization after amide-A band excitation. A single exponential fit with the time constant of 4.2 ± 0.5 ps is shown.

Decay kinetics at bleach (3292 cm^{-1}) and new absorption (3430 cm^{-1}) peaks can be fitted satisfactory by a single exponential function with the decay times of 4.2 ± 0.5 and 3.8 ± 0.5 ps, respectively. However, a better fit is obtained with two exponentials; for example, for the decay at 3292 cm^{-1}, the decay times are 2.4 ± 1 and 6.3 ± 1.7 ps, with relative amplitudes of 1.3 ± 0.8 and 1.5 ± 0.9, respectively. This suggests the presence of several structures with nonequal T_1 values. However, the error bars for the decay times are large; therefore, only the averaged value of 4 ps is presented in Table 1. The transient spectra continue to show the diagonal anharmonicity of 144 cm^{-1} throughout the T_1 decay, proving that the N−H mode remains populated and that the measured dynamics corresponds to the excited amide-A mode. The long lifetime of the amide-A mode provides a large observation time window to monitor the off-diagonal cross-peaks so that reliable off-diagonal anharmonicity values are obtained from global fits.

Cross-Peak Region. A slightly broadened bleach band (1679 cm^{-1}) and one relatively broad new absorption band (maximum at 1652 cm^{-1}) are found in the cross-peak region (Figure 10). The direct coupling between amide-A and amide-I in a single amide unit is clearly observed in this case free from the relaxation process that is present for AcAla(D)OMe. Similarly to AcAla(D)OMe, two subbands are required to fit the data. The main band at 1677 cm^{-1} exhibits an off-diagonal anharmonicity of 1.4 ± 0.4 cm^{-1}, while the weak subband at the low-frequency side (1665 cm^{-1}) has a larger anharmonicity of 2.6 ± 0.8 cm^{-1}. The anharmonic coupling between N−H and amide-I (main components) (1.4 cm^{-1}) is close to that found
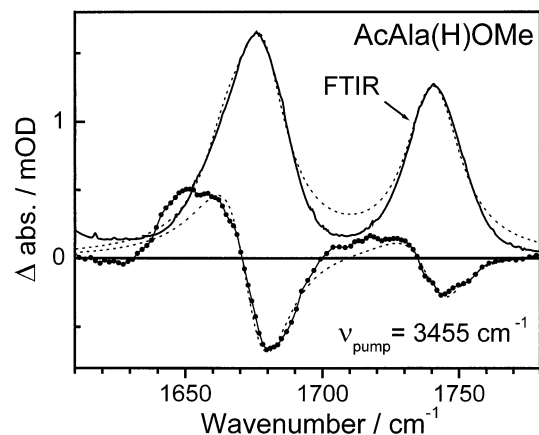

Figure 10. Magic angle transient spectra for AcAla(H)OMe in the amide-I/C=O stretch band region (line with dots) measured at 350 fs time delay after excitation of the amide-A mode along with the FTIR absorption spectrum (thick solid line). The fits of the transient and linear spectra are shown by dashed lines.
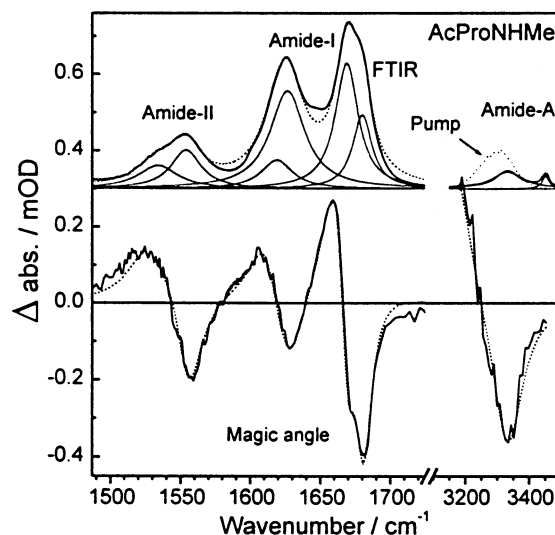

Figure 11. Magic angle transient spectra for AcProNHMe measured at 200 fs time delay after excitation of the hydrogen-bonded amide-A mode along with the FTIR absorption (with deconvoluted components) and the pump laser spectrum (upper panel). Dashed lines show fits of the transient and linear spectra.

for the deuterated compound (1.6 cm^{-1}). This result is interesting considering that the N−H motion is more localized than that of N−D. The coupling of the amide-A mode and the ester carbonyl is also determined from the magic angle data such as that in Figure 10, at 1.2 ± 0.3 cm^{-1}. However, the anisotropy is found to be not constant across this band, implying existence of more than one conformation. As discussed in Section 4.6, these conformers have different anharmonicity values.

3.2.3. Coupling of the Amide-A and Amide-I Modes in the C_7 Conformation of AcProNHMe. Diagonal Peaks. In this experiment, the pump pulse predominantly excites the internally H-bonded C_7 conformational distribution of the peptide. The transient spectra in the amide-A spectral region shown in Figure 11 exhibit a bleach and new absorption anharmonically shifted by 165 ± 15 cm^{-1}. The population relaxation time of the N−H mode is found to be 585 ± 60 fs (data are not shown).

Cross-Peak Region: On the Same Amide. The transient peaks in the spectral range of both amide-I bands of AcProNHMe are observed (see Figure 11). The spectrum at the amide-I (methyl-amino end) band near 1670 cm^{-1} shows the same substructure as seen in the linear spectrum. The same off-diagonal anhar-

Vibrational Coupling between Amide-I and Amide-A Modes

J. Phys. Chem. A, Vol. 107, No. 18, 2003 **3391**

monicity of 3.5 cm^{-1} is found for each subband coupled to the methylamino N$-$H band. The coupling of the amide-A and amide-I on the methylamino end of the peptide is about twice that found for AcAlaOMe.

Cross-Peak Region: Across the Hydrogen Bond. The transient signal at ~1620 cm^{-1} arises from the coupling of amide-A and the acetyl end amide-I mode that are spatially separated by the hydrogen bond of the C$_7$ conformation. Two components are necessary to fit the linear and transient spectra (see Section 3.1 and Figure 11). The dominant component at higher frequency (1626 cm^{-1}) has the C$_7$ amide-A/amide-I off-diagonal anharmonicity of 1.4 ± 0.4 cm^{-1} (see Table 1). The minor component at 1619 cm^{-1}, which is probably caused by Fermi resonance, has a larger off-diagonal anharmonicity of 5.5 ± 1 cm^{-1}.

3.2.4. Coupling of the Amide-A and Amide-II Modes in AcProNHMe. The transient signal at the amide-II (methylamino end) band position after pumping the N$-$H stretch is also observed (see Figure 11). The fitting of the transient spectra required the inclusion of two components: a dominant one with anharmonicity of 2.5 ± 0.8 cm^{-1} and a small contribution (20%) with a large anharmonicity of ~20 cm^{-1}. We ascribe the dominant component of 2.5 cm^{-1} to the anharmonic coupling between the amide-A and the amide-II modes. The other component is considered to arise after energy transfer between the amide-A and the amide-II bands both localized at the methylamino end of the peptide. The large anharmonicity would then arise from the population in the amide-II mode. About 30% of the excited amide-A mode population has decayed at the delay time of 200 fs, when the spectrum of Figure 11 was measured.

3.3. Transition Moment Orientation and Geometric Information. The angular relationships between vibrators were studied by polarization anisotropy measurements, which were performed by changing the polarization of probe with respect to that of the pump. The characteristic rotation times of these dipeptides are about 6$-$10 ps[1,36] so the depolarization caused by overall rotation of the molecule is negligible at time delays in the range of 200 fs at which the early time spectra are reported. The polarization ratio, $\alpha = S_{\parallel}/S_{\perp}$, or the anisotropy $r = (S_{\parallel} - S_{\perp})/(S_{\parallel} + 2S_{\perp})$, therefore relate to a mean square cosine:

$$\langle \cos^2 \xi_{ij} \rangle = \frac{2\alpha - 1}{\alpha + 2} = \frac{5r + 1}{3} \tag{1}$$

in which ξ_{ij} is the angle between the transition dipole moments of the modes i and j and the average is over the distribution of molecular structures. The signals with pump and probe polarization parallel and perpendicular are $S_{\parallel}$ and $S_{\perp}$. The angles referred to in the text are $\theta_{ij} = \cos^{-1}(\sqrt{\langle \cos^2 \xi_{ij} \rangle})$ and $-\theta_{ij}$, the latter arising because the experiment does not distinguish between θ which is on line with $\pi + \theta$, and $\pi - \theta$ which is on line with $-\theta$, so it measures two possible alignments of the pairs of transition moments.

Representative parallel and perpendicular components $S_{\parallel}$ and $S_{\perp}$ are shown in Figure 12 for AcAlaOMe (D) and (H). For both compounds, the anisotropy is practically constant across the probed amide-I band near 1680 cm^{-1}. In contrast, the anisotropy is not constant near the carbonyl mode at the ester end near 1750 cm^{-1}, indicating that more than one structure involving the ester group is contributing to the signal. The variation of anisotropy is similar for both isotopomers, but a detailed analysis was carried out only for AcAla(H)OMe.

As described before for AcAlaOMe (see Figure 3B), the small and narrow shoulder at 3451.6 cm^{-1} was assigned to a
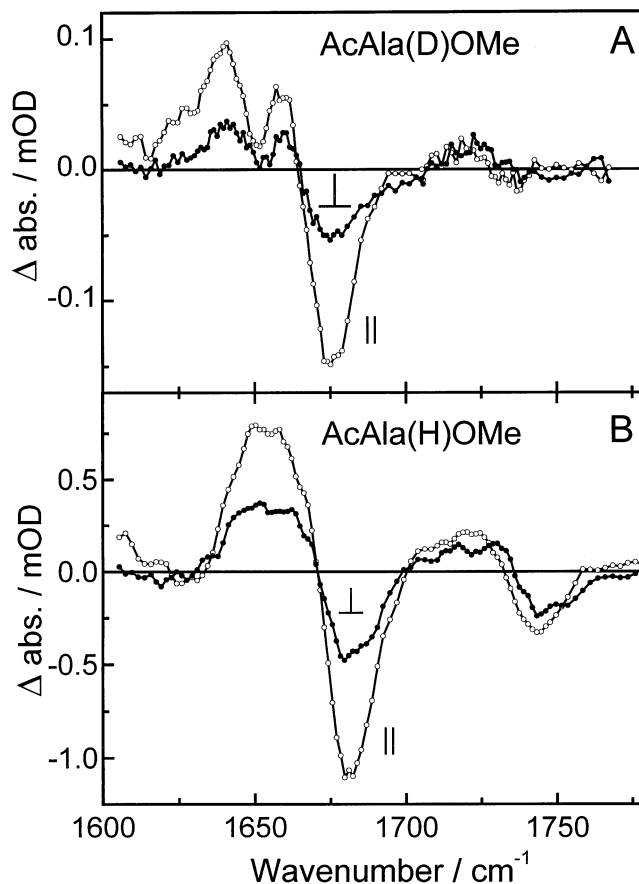

Figure 12. Polarized transient spectra in the amide-I region for AcAla-(D)OMe at 0 fs delay (A) and AcAla(H)OMe at 350 fs (B) after amide-A band excitation. The spectra of the respective pump pulses are shown in Figure 3. The polarization of the probe is tuned to parallel (||, opened circles) or perpendicular ($\perp$, filled circles) to the pump polarization.

conformer where the N$-$H group is not hydrogen-bonded. This conformer contributes only to about 12.5% of all existing structures at this concentration as calculated from the areas. Therefore, to account for the observed $S_{\parallel}$ and $S_{\perp}$, spectral components of two more conformations have to be included. To fit the data, these two structures must have carbonyl bands significantly shifted with respect to each other and different angles between the carbonyl and the N$-$H groups. Particularly, the conformer with the red-shifted carbonyl band should have high positive anisotropy, while the conformer with the carbonyl band at higher frequency should have negative anisotropy. It turns out that to fit the data the carbonyl frequency of the red-shifted band should be at ca. 1730$-$1734 cm^{-1}, which is significantly shifted from the band maximum (by ca. 10 cm^{-1}), and the band should be broadened. This limits the contribution from this conformer to ca. 35%, which makes the conformer with the carbonyl band at higher frequency a dominant conformer.

The combined fit results of the off-diagonal transient spectra with parallel and perpendicular polarizations, the diagonal amide-A magic angle transient spectrum, and the linear spectrum are shown in Figure 13. The conformer with the free N$-$H groups was assumed to have a carbonyl frequency at the high-frequency side of the band (1747.5 cm^{-1}, fwhm = 16 cm^{-1}); this assignment, however, does not affect the conclusions, as the contribution of these structures is small. The fit required the anisotropies to be -0.13 ± 0.07 and 0.3 ± 0.1, respectively, for the C=O bands at 1741.7 ± 1 and 1734 ± 2 cm^{-1} with
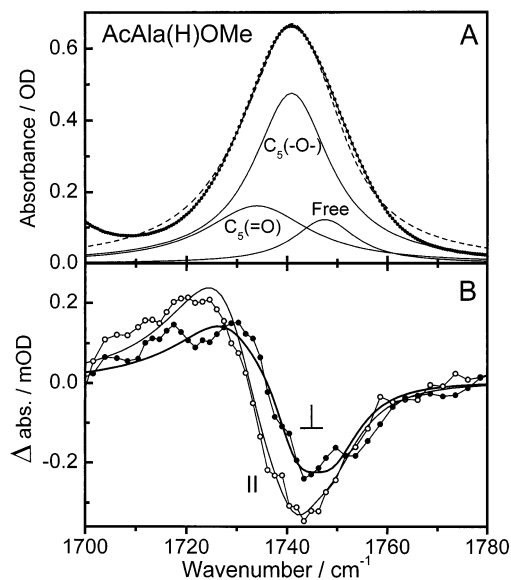
Figure 13. Linear absorption spectrum with deconvoluted components (A) and polarized transient spectra (B) of AcAla(H)OMe in the carbonyl band region. The solid lines in B are the fits.
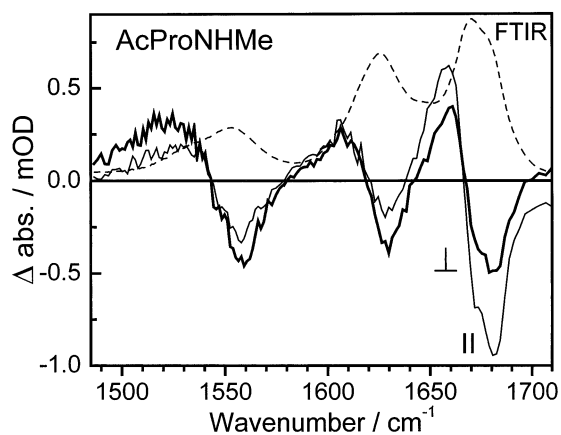

Figure 14. Polarized transient spectra in the amide-I/amide-II band regions for AcProNHMe, 200 fs after amide-A band excitation along with the linear spectrum (dashed line). The spectrum of the pump pulses is shown in panel C.

widths 19 ± 2 and 25 ± 2 cm^{-1}. Naturally, the off-diagonal anharmonicities have larger uncertainties, being $0.3-1$, $1.8-3$, and $0.4-1.1$ cm^{-1} for the bands at 1741.7, 1734, and 1747.5 cm^{-1}, respectively. The assignment of these two structures is presented in Section 4.6.

The off-diagonal polarized transient spectra of the AcProN-HMe show practically constant anisotropy across each of the three probed bands: amide-I (amino end), amide-I (acetyl end), and amide-II (amino end) (Figure 14). This confirms that dominantly the C$_7$ conformers are excited in that case.

4. Discussion

The N—H vibrational mode of peptides and polypeptides is highly localized, being almost a pure N—H stretching motion. Its diagonal anharmonicity in the range of 150 cm^{-1} makes it a very anharmonic motion as compared with other amide modes. The N—H mode region is also very sensitive to molecular structure, but the complexity of its Fermi resonances with combination bands and overtones has resulted in the amide-I region being more widely used in structural studies. In order that the N—H and N—D modes are rendered more useful in multidimensional spectroscopies, it is necessary to obtain

information on their coupling to other amide modes. The energy for a pair of amide-A and amide-I region modes, up to second order in their vibrational quantum numbers v_A and v_I, is

$$G(v_A, v_I) = \omega_A(v_A + {}^1/_2) + \chi_{AA}(v_A + {}^1/_2)^2 + \omega_I(v_I + {}^1/_2) + \chi_{II}(v_I + {}^1/_2)^2 + \chi_{AI}(v_A + {}^1/_2)(v_I + {}^1/_2)$$

where ω_A and ω_I are the zero order frequencies and χ_{ij} is the anharmonicity. In the present notation, the fundamental frequencies are $\omega_{A0} = G(1,0) - G(0,0)$ and $\omega_{I0} = G(0,1) - G(0,0)$; the 1→2 transitions are at $\omega_{A0} - \Delta_A$ and $\omega_{I0} - \Delta_I$ where the diagonal anharmonicity is, for example, $\Delta_A = -2\chi_{AA} - 1/2\chi_{AI}$; and the combination band frequency is $\omega_{A0} + \omega_{I0} - \Delta_{AI}$. The off-diagonal anharmonicity is $\Delta_{AI} = -\chi_{AI}$. We also refer to Δ_{AI} as the mode coupling. Both mechanical interactions and through space electrostatic effects will contribute to the mode coupling. Sometimes, these contributions can be treated separately.[27] We have generated models for the anharmonicities in peptides with spatially separated amides based on through space electrostatic interactions.[7,52,53] For amide units that are adjacent to one another in polypeptides, the mechanical coupling, or through bond forces, is likely to be the dominant contribution[30,36,52] so coupling models will require other modes to be involved. As far as we know, no simple model for the coupling constant χ_{AI} has been reported.

4.1. Substructure of Bands. For the amide-I and amide-A bands that are examined here, more than one transition is often seen in the region of interest even though the molecule contains only one amide group. Accidental degeneracies (Fermi resonances), multiple conformations of the peptides, or the presence of aggregates of the peptide can cause these additional bands. The occurrence of Fermi resonances in the spectra of carbonyls and N—H stretch modes is well-known: in fact, the strong carbonyl stretch IR transitions are seldom ever found as single symmetric bands and nearby combination bands are often intensified.

In the case of AcAlaOMe, the presence of two amide-I band components at 1678 and 1665 cm^{-1} (1670 and 1650 cm^{-1} for the deuterated compound) is probably a result of Fermi resonance. The extra band is unlikely to be caused by the presence of a subpopulation of a hydrogen-bonded conformation since this structure would introduce a coupling of the N—D(H) and the Ala C=O at 1740 cm^{-1}. The Fermi resonance hypothesis is consistent with the observed significant difference between the off-diagonal anharmonicities of the a and b amide-I components in combination with the amide-A mode for both isotopomers (see Table 1); we expect that the off-diagonal anharmonicity of a combination band would be dominated by properties of the combining modes, not necessarily by the amide mode providing the intensity. On the contrary, the substructure of the amide-A band in AcAlaOMe, most clearly evident in the H-form (see Figure 3B), is attributed to different conformations, as discussed in Section 4.6.

4.2. Simulations and Global Fitting of Data. For simulations of the data, dephasing times (see Table 1) were obtained from the linear IR or transient spectra. The population relaxation times (T_1) were either measured from the diagonal pump/probe experiments or assumed from previous studies of model amide-I mode relaxation that showed the relative insensitivity of the amide-I relaxation to structure.[1] The relaxation times of higher excited states were estimated from harmonic models. The fitting was done by calculating the response functions based on these parameters, carrying out the appropriate convolutions with the driving fields and Fourier transforming along the time axis after

Vibrational Coupling between Amide-I and Amide-A Modes

J. Phys. Chem. A, Vol. 107, No. 18, 2003 **3393**

the third field interaction to calculate the pump/probe spectrum. The linear spectrum of AcAla(D)OMe was calculated by assuming a homogeneous line width for both a and b components in the amide-I mode and for the amide-A mode. The simulated spectra fit the experimental results reasonably (Figure 6). The simulated off-diagonal cross-peak spectra (thick solid lines) are superimposed on the experimentally obtained transient spectra at similar delay times in Figure 6, and satisfactory agreement is found between the calculated and measured data.

In Figure 8, the signal at negative delay time (probe before pump) contains the perturbed IR free induction decay,[45,46] which is determined by the inverse of the total width of the absorption band. The small discrepancy near zero time delay between experiment and simulation is from the contribution of solvent present in the experimental data (see Experimental Section). The data were fit by assuming the two subpopulations (amide-A and x) having different anharmonic couplings to the amide-I mode. The solid lines through the data points in Figure 7 correspond to this global fit, which yields the two anharmonic couplings and the relaxation times. Because the relaxation out of the N—D mode is comparable with the time resolution, 40% of the observed signal at zero time delay is due to the intermode coupling between a relaxed mode or modes and the amide-I mode. The time-dependent apparent off-diagonal anharmonicity can also be simulated from first principles by including the diagrams involving x shown in Figure 2. The fitting requires the coupling between the x modes and amide-I to be stronger than between amide-A and amide-I. For the N—H peptide, the apparent coupling is not initially time-dependent: as a result of the much longer lifetime of N—H as compared with N—D, the vibrational relaxation does not influence the signals significantly in this case and the off-diagonal anharmonicity is measured directly and free from interference from the transitions of other modes.

4.3. Angular Properties. As described above, the anisotropy measurements yield the transition dipole alignments. The alignments of the transition dipole moments of the amide-A and amide-I (C=O) in the same amide unit are found to be different for different peptides (see Table 1). For example, we find values for θ_{ij} of $\pm 20°$ (± 3) in AcAlaOMe and $\pm 35°$ (± 3) in AcProNHMe. This indicates a diversity in the angular relationship between the N—H and the C=O groups in different molecular environments, in agreement with previous results.[22,28,54] We also found that the alignment depends on N—H/N—D exchange: the angle θ_{ij} is $\pm 20 \pm 3°$ in the N—H form and $\pm 13 \pm 4°$ in the N—D form. Because the amide-A mode is a localized vibrator, its transition dipole moment direction must be close to the N—H bond axis[21] and we will assume in the ensuing discussion that it is precisely along the N—H axis. The deuterated amide-A transition dipole is also assumed to be along the N—D bond axis although, because of its proximity to the mid-IR fundamentals and the mass change, the mode should not be as localized as N—H. On the otherhand, it is well-known that the direction of the transition dipole moment of the amide-I mode is not parallel to the C=O bond axis.[21,27]

Amide groups in proteins generally adopt planar conformations[55] because of the partial double bond character of the C—N bond.[56] Both isolated amides and those participating in external hydrogen bonding are planar ($\omega \geq 178°$)[56,57] with average angles, $\angle OCN = 123.2°$, $\angle CNH = 119.5°$, and $\angle CO,NH = 3.7°$,[57] which are very close to the angles calculated at the ab initio 6-31G* level for the AcAlaOMe dipeptide ($\angle OCN = 122.4°$, $\angle CNH = 119.8°$, and $\angle CO,NH = 2.6°$). The γ-turn structure discussed herein is an example where the amide can

be less planar ($\omega \sim 173-175°$) due to the strain involved in forming a seven-membered ring in the self-hydrogen-bonded conformation.[58,59]

To clarify the discussion of transition dipole alignments, we define a right-handed coordinate system with z along the N→H or N→D bond axis, y pointing toward the carbonyl end of the amide group and x perpendicular to the plane of the amide group. For AcAla(D)OMe, the measurement locates the amide-I transition dipole at either of the polar angles $\theta = 13$ or $180-13°$, both with $\phi = \pi/2$. The latter choice is consistent with the calculations and measurements of Krimm and co-workers (ref 21 and references therein). The C=O bond axis has the polar angle $(180-3) = 177°$ ($\phi = \pi/2$) according to numerous experiments and calculations.[21,57,59] On this basis, the amide-I transition moment is measured to be 10° to the C=O axis.

Both the a and the b amide-I band regions of AcAla(D)OMe exhibit the same cross-peak anisotropy; therefore, they have the same alignments of amide-A and amide-I. This is again consistent with them being Fermi resonances. This alignment of the N—H and amide-I transition dipoles for AcAla(D)OMe was found to be $157 \pm 3°$ ($\phi = \pi/2$), yielding an angle of $20 \pm 3°$ between the amide-I transition dipole and the C=O bond, which agrees well with the value of 20° obtained from theory.[21] Both the a and the b subbands of the amino end amide-I of AcProNHMe also show the same alignment to the amide-A mode dipole (see Table 1). On the basis of the above discussion, the angle between the transition moments is identified as $145.5 \pm 3°$ ($\phi = \pi/2$). The N—H of AcProNHMe participates in an intramolecular H-bonded seven ring C_7 structure. However, in this case, the value of 34.5° for the alignment of the amide-I transition dipole and the C=O group is 11.5°, larger than found for the isolated amide (AcAla(H)OMe). The angle of the NH group to the CO group in the C_7 conformation is computed as 8.5°,[59] which suggests that the amide-I transition dipole is rotated to be 25° to the C=O bond axis in the H-bonded structure.

The amide-II (methylamine end) transition dipole is aligned at $75 \pm 3°$ to the amide-A mode dipole in AcProNHMe. The computed angle between the CN and the NH bonds in the C_7 structure is 63°[59] so the amide-II transition dipole must make an angle of 12° to the CN bond direction. This is close to the value of 73° previously reported for the angle between the amide-II transition dipole and the C=O bond.[21]

For AcProNHMe, the acetyl amide-I band shape is asymmetric but the transient anisotropy is again constant across the band giving an angle θ_{ij} between the N—H and the amide-I transition moments of $\pm 64 \pm 4°$ (see Table 1). The angle between NH and CO bonds is calculated at the ab initio 6-31G* level to be 69-72° in the C_7 self-H-bonded structure. If the amide-I transition moment was assumed to be at 20° to the CO bond, the angle between the amide-I and the amide-A dipoles would be 52°. An angle of 7-10° instead of 20° for the amide-I dipole/C=O bond alignment gives good agreement of the anisotropy data. This result suggests that the amide-I mode transition dipole may be more parallel to the CO bond for proline as compared with other peptides.

4.4. Coupling Magnitudes. The N—H and N—D stretching modes are considered to be localized, and this is consistent with their frequencies: if the modes involved only two atoms, the zero order frequencies would exhibit a deuterium isotope downshift of 27%, as compared with an observed value of 24%. For a Morse potential, the cubic anharmonicity is inversely proportional to the reduced mass predicting a ratio $\Delta_A(H)/\Delta_A(D) = 1.89$ whereas we measure a change in the right direction but only a factor of 1.36. It could be that the force fields are

not the same for the isotopomers, consistent with the transition dipole directions being different, or just that the Morse model is too inaccurate. However, there is at least an indication that ND is not so localized as N−H. The diagonal anharmonicity of the N−H mode is approximately the same in two different peptides AcAlaOMe and AcProNHMe, which is again useful information for modeling potential surfaces and 2D IR spectroscopy.

The coupling D_{AI} of the N−H and amide-I modes across the H-bond is determined for AcProNHMe in the C_7 conformation to be 1.4 ± 0.4 cm^{-1} (Table 1). The coupling of the N−H mode in AcProNHMe with the acetyl carbonyl is comparable with its coupling to the carbonyl (amide-I) associated with the same amide group. This anharmonic coupling must derive from the C=O- - -H−N potential function since there is unlikely to be any significant coupling of these groups through the backbone. All of the couplings are comparatively small presumably because of the localized character of the N−H bond mode. However, no simple model for these couplings seems apparent at this time although they represent a significant challenge to modern computational methods of determining the potential energy surfaces of peptides and hydrogen-bonded peptides. These anharmonic couplings are also essential parameters for the development of models needed to interpret multidimensional infrared spectra.[53]

The anharmonic coupling between the amide-I and the amide-A modes in the same amide group is similar for the two AcAlaOMe isotopomers. This result is consistent with the three state model in which the NH−CO (or ND−CO) combination band couples to both the NH (or ND) and amide-I overtones through a bilinear interaction. Such a model predicts an anharmonic shift of

$$\Delta_{AI} = \frac{-2\beta^2(\Delta_A + \Delta_I)}{(E_A - E_I - \Delta_A)(E_A - E_I + \Delta_I)}$$

where β is the coupling. The experimental values of Δ_{AI} predict $\beta = 113$ and 67 cm^{-1} for N−H and N−D isotopomers, respectively. The fact that the N−D mode has the smaller transition dipole moment and that the implied coupling magnitudes are in the few tens of cm^{-1} range suggest that there is a substantial electrostatic contribution to β. However, this model is greatly oversimplified and there is as yet insufficient data available to provide a thorough test.

4.5. Relaxation Dynamics. The N−H modes of AcProNHMe and AcAlaOMe have remarkably different values of T_1 with the AcAlaOMe, N−H relaxation being almost 10 times faster (see Table 1). In both peptides, the nitrogen atom is directly bonded to a carbonyl and to a saturated carbon atom, which for one case is the α-carbon of the alanyl and for the other it is a methyl group. Because these N−H environments are similar, we could have expected them to exert comparable forces on the N−H bond and lead to similar relaxation times. A major structural difference between the two is that in acetylproline the structure is an internally hydrogen-bonded C_7 configuration.[11,18,36,50] Therefore, it is suggested that the H-bonding to the acetyl C=O in the acetylproline shortens the N−H lifetime by an order of magnitude. There is precedent for the effect of H-bonding on vibrational relaxation of N−H modes through the work of Heilweil and co-workers on pyrrole.[60]

The decay of the transient bleach signal (2550 cm^{-1}) in AcAla(D)OMe exhibits two exponentials with components of 570 ± 40 fs (91%) and 5.5 ± 0.8 ps (9%), while the transient absorption signal at 2450 cm^{-1} is exponential with a decay time

of 610 ± 60 fs (Figure 4). The fast component clearly corresponds to the lifetime of the excited amide-A mode, and the slow component in the bleach signal decay is assigned to the relaxation of the other modes that are coupled to the amide-A mode. In a recent paper,[36] we showed that a nonexponential decay of the amide-I mode can be caused by a fast relaxation to other modes, which then decay more slowly. These distinctions can be made only when the probe spectrum is measured as a function of delay, and they dramatize the possible pitfalls of single pulse pump/probe experiments. The effect is clearer for the amide-A mode whose diagonal anharmonicity is much larger than the off-diagonal anharmonicities. As a result, the diagonal and off-diagonal signals are overlapping only at the bleach spectral region $|00\rangle \rightarrow |01\rangle$ but not at the spectral region of the new absorptions $|01\rangle \rightarrow |02\rangle$ and $|00x\rangle \rightarrow |01x\rangle$ (Figure 2). Thus, different decay dynamics are expected at the bleach ($|00\rangle \rightarrow |01\rangle$) and new absorption ($|01\rangle \rightarrow |02\rangle$) frequencies, in agreement with our observations. The slow component of 5.5 ps thus belongs to the relaxation dynamics of the x group of states. This effect is not pronounced for AcAla(H)OMe where the average amide-A band lifetime is long (4 ps) and not very different from the relaxation times of other states.

The observation of a significant effect of deuteration on the T_1 relaxation of AcAlaOMe has not been quantitatively rationalized. However, qualitatively, it is not unexpected. The N−D mode is less local than N−H and hence is more effectively coupled to displacements of neighboring atoms thereby providing more effective pathways of relaxation. Furthermore, because of its lower frequency than N−H, it can relax through fewer numbers of quanta of accepting modes. Quite different effects have been reported for the O−D mode. It relaxes more slowly than O−H in liquid water.[61] The O−H and O−D vibrational relaxations for a number of alcohols and silanols are very similar[32] and have much longer lifetimes than we find for N−H or N−D. The N−H mode of free pyrrole relaxes in 50 ps, much longer than observed in the present work[60,62] although in that example it was found that the N−D stretch mode relaxed much more rapidly.[60] Clearly, the N−H and N−D modes of peptides are significantly more strongly coupled to other modes than the N−H, the O−H, or the O−D in these examples, perhaps with the exception of the N−D mode of pyrrole.

The spectral width of 62 cm^{-1} for the transient absorption ($|01\rangle \rightarrow |02\rangle$) of AcAlaOMe at ~3290 cm^{-1} is about twice that of the ground state absorption ($|00\rangle \rightarrow |01\rangle$) width of 33 cm^{-1} but less than the 125 cm^{-1} width found for the transient absorption band of the amide-A(D) mode. According to the theory of anharmonicity-induced dephasing,[63] all of the one quantum transitions should have the same width from pure dephasing so this is unlikely to be the effect that is observed. Therefore, we conclude that these line width changes reflect, at least in part, large changes of T_1. This is supported by the expectations for an harmonic oscillator where the line width of the 0→1 transition contains a contribution from population decay of $1/2T_1$, which increases to $3/2T_1$ for the 1→2 transition.

4.6. Analysis of the AcAlaOMe Conformations. The results that provide the essential clues to the nature of the AcAlaOMe structures present in the solution are the amide-A and amide-I band frequencies and the anisotropy induced in the ester C=O transition by pumping the amide-A band. The amide-A frequency at 3435 cm^{-1} is significantly shifted from the free N−H region at 3450−3460 cm^{-1}. A probable cause of this N−H frequency shift is a H-bonding in a five ring structure (C_5).[18] This conclusion is firm because other possible causes of the shift such as aggregation or hydrogen bonding to the solvent
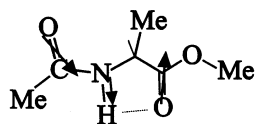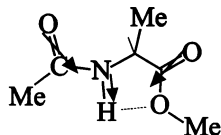
Vibrational Coupling between Amide-I and Amide-A Modes

J. Phys. Chem. A, Vol. 107, No. 18, 2003 **3395**

C_5(carbonyl) conformer

C_5(ester) conformer

Figure 15. Skeletal diagram of AcAlaOMe in two conformations: C_5 (carbonyl) and C_5 (ester). Arrows indicate the measured directions of the amide-A, amide-I, and ester carbonyl transition dipoles.

are eliminated. There are two possible C_5 structures for AcAlaOMe: the one caused by interaction of the N=H with the ester C=O (C_5(carbonyl)) and the other where N=H interacts with the ester oxygen (C_5(ester)) (Figure 14).

The ester carbonyl band anisotropy shows that the frequency for one conformer is significantly downshifted, suggesting that the carbonyl group is involved in hydrogen bonding. The high positive anisotropy of ca. 0.3 observed for this structure indicates that C=O and N—H transition dipoles are close to being parallel and allows us to assign this structure to C_5 (carbonyl). However, the carbonyl band anisotropy in the second conformer is negative and is not downshifted, indicating that the carbonyl is not participating in hydrogen bonding. This structure is assigned to the C_5 (ester), where the ester C=O and N—H bond axes make a large angle. The angle between the N—H and the carbonyl (ester end) bonds of 69° calculated at the ab initio 6-31G* level falls into the range determined experimentally of 62—90° for the dominant conformer (Table 1). The results of fitting the data show that the populations of the C_5 (carbonyl) and C_5 (ester) conformers are similar, suggesting that they have similar hydrogen bond strength and that both of these structures contribute to the N—H mode in the 3435 cm^{-1} region.

The off-diagonal anharmonicity is larger for the C_5 (carbonyl) conformer (Table 1). With reference to the structure in Figure 15, the larger off-diagonal anharmonicity for the C_5 (carbonyl) is consistent with the absence of direct bonding between the N—H and the C=O groups in the C_5 (ester) conformer. The alignment of the transition dipoles in the C_5 (carbonyl) also favors a larger through space electrostatic interaction for that case.

5. Summary

We have shown that two color infrared pump/probe spectroscopy is an effective approach for obtaining the vibrational coupling between amide-I and amide-A modes in small peptides. The intermode anharmonic coupling constants have been measured to be in the range of a few cm^{-1}. The vibrational relaxation-induced intermode coupling was also revealed from the time-dependent spectral shifts. The vibrational lifetime of the amide-A mode is shortened upon forming an intramolecular hydrogen bond. The alignments of the transition dipole moments of amide-A and amide-I modes are found to depend on molecular structure and on hydrogen bonding, consistent with previous experimental results and theoretical calculations. The two color transient spectra can be calculated and fit satisfactorily to experimental data.

References and Notes

(1) Hamm, P.; Lim, M.; Hochstrasser, R. M. *J. Phys. Chem. B* **1998**, *102*, 6123.

(2) Asplund, M. C.; Zanni, M. T.; Hochstrasser, R. M. *Proc. Natl. Acad. Sci. U.S.A.* **2000**, *97*, 8219.

(3) Woutersen, S.; Hamm, P. *J. Phys. Chem. B* **2000**, *104*, 11316.

(4) Piryatinski, A.; Tretiak, S.; Chernyak, V.; Mukamel, S. *J. Raman Spectrosc.* **2000**, *31*, 125.

(5) Zanni, M. T.; Asplund, M. C.; Hochstrasser, R. M. *J. Chem. Phys.* **2001**, *114*, 4579.

(6) Zanni, M. T.; Hochstrasser, R. M. *Curr. Opin. Struct. Biol.* **2001**, *11*, 516.

(7) Gnanakaran, S.; Hochstrasser, R. M. *J. Am. Chem. Soc.* **2001**, *123*, 12886.

(8) Scheurer, C.; Piryatinski, A.; Mukamel, S. *J. Am. Chem. Soc.* **2001**, *123*, 3114.

(9) Ge, N.-H.; Hochstrasser, R. M. *Phys. Chem. Commun.* **2002**, *3*, 1.

(10) Hochstrasser, R. M. *Chem. Phys.* **2001**, *266*, 273.

(11) Zanni, M. T.; Gnanakaran, S.; Stenger, J.; Hochstrasser, R. M. *J. Phys. Chem. B* **2001**, *105*, 6520.

(12) Ge, N.-H.; Zanni, M. T.; Hochstrasser, R. M. *J. Phys. Chem. B* **2002**, *106*, 962.

(13) Mukamel, S. *Principles of Nonlinear Spectroscopy*; Oxford University Press: New York, 1995.

(14) Woutersen, S.; U., E.; Bakker, H. J. *Science* **1997**, *278*, 658.

(15) Laenen, R.; Gale, G. M.; Lascoux, N. *J. Phys. Chem. A* **1999**, *103*, 10708.

(16) West, W., Ed. *Chemical Applications of Spectroscopy*; Interscience Publishers, Inc.: New York, 1956.

(17) Miyazawa, T. *J. Mol. Spectrosc.* **1960**, *4*, 168.

(18) Neel, J. *Pure Appl. Chem.* **1972**, *31*, 201.

(19) Tonan, K.; Ikawa, S. *J. Am. Chem. Soc.* **1996**, *118*, 6960.

(20) McQuade, D. T.; McKay, S. L.; Powell, D. R.; Gellman, S. H. *J. Am. Chem. Soc.* **1997**, *119*, 8528.

(21) Krimm, S.; Bandekar, J. *Adv. Protein Chem.* **1986**, *38*, 181.

(22) Bradbury, E. M.; Elliott, A. *Spectrochim. Acta* **1963**, *19*, 995.

(23) Miyazawa, T. *Aspects Protein Struct., Proc. Symp., Madras* **1963**, 257.

(24) Miyazawa, T.; Blott, E. R. *J. Am. Chem. Soc.* **1961**, *83*, 712.

(25) Rey-Lafon, M.; Forel, M. T.; Garrigou-Lagrange, C. *Spectrochim. Acta, Part A* **1973**, *29*, 471.

(26) Dwivedi; Krimm, S. *Macromolecules* **1982**, *15*, 177.

(27) Torii, H.; Tasumi, M. *J. Chem. Phys.* **1992**, *96*, 3379.

(28) Abbott, N. B.; Elloit, A. *Proc. R. Soc. A* **1956**, *234*, 247.

(29) Hamm, P.; Lim, M.; DeGrado, W. F.; Hochstrasser, R. M. *J. Chem. Phys.* **2000**, *112*, 1907.

(30) Woutersen, S.; Hamm, P. *J. Chem. Phys.* **2001**, *114*, 2727.

(31) Heilweil, E. J.; Moore, R.; Rothenberger, G.; Velsko, S.; Hochstrasser, R. M. *Laser Chem.* **1983**, *3*, 109.

(32) Heilweil, E. J.; Cassassa, M. P.; Cavangah, R. R.; Stephenson, J. C. *J. Chem. Phys.* **1986**, *85*, 5004.

(33) Owrutsky, J. C.; Li, M., Culver, J. P., Sarisky, M. J., Yodh, A. G., Hochstrasser, R. H., Eds. *Vibrational Dynamics of Condensed-Phase Molecules Studied by Ultrafast Infrared Spectroscopy*; 1994; Vol. 74.

(34) Lim, M.; Hochstrasser, R. M. *J. Chem. Phys.* **2001**, *115*, 7629.

(35) Laubereau, A.; Kaiser, W. *Rev. Mod. Phys.* **1978**, *50*, 607.

(36) Rubtsov, I. V.; Hochstrasser, R. M. *J. Phys. Chem. B* **2002**, *106*, 9165—9171.

(37) Rubtsov, I. V.; Wang, J.-P.; Hochstrasser, R. M. *The 13th International Conference on Ultrafast Phenomena*; Vancouver, Canada, 2002.

(38) Graener, H.; Ye, T. Q.; Laubereau, A. *J. Chem. Phys.* **1989**, *91*, 1043.

(39) Graener, H.; Laubereau, A. *J. Phys. Chem.* **1991**, *95*, 3447.

(40) Dlott, D. D. *Abstr. Pap. J. Am. Chem. Soc.* **2000**, *220*, PHYS.

(41) Owrutsky, J. C.; Culver, J. P.; Li, M.; Kim, Y. R.; Sarisky, M. J.; Yeganeh, M. S.; Hochstrasser, R. M.; Yodh, A. G. *Springer Ser. Chem. Phys.* **1993**, *55*, 345.

(42) Fujino, T.; Kashitani, M.; Onda, K.; Wada, A.; Domen, K.; Hirose, C.; Ishida, M.; Goto, F.; Kano, S. S. *J. Chem. Phys.* **1998**, *109*, 2460.

(43) Onda, K.; Tanabe, K.; Noguchi, H.; Wada, A.; Shido, T.; Yamaguchi, A.; Iwasawa, Y. *J. Phys. Chem. B* **2001**, *105*, 11456.

(44) Germer, T. A.; Stephenson, J. C.; Heilweil, E. J.; Cavangah, R. R. *Phys. Rev. Lett.* **1993**, *71*, 3327.

(45) Wynne, K.; Hochstrasser, R. M. *Chem. Phys.* **1995**, *193*, 211.

(46) Hamm, P. *Chem. Phys.* **1995**, *200*, 415.

(47) Bratos, S.; Leicknam, J. C. *J. Mol. Liq.* **1995**, *64*, 151.

(48) Laenen, R.; Simeonidis, K. *Chem. Phys. Lett.* **1999**, *299*, 589.

(49) Owrutsky, J. C.; Li, M.; Locke, B.; Hochstrasser, R. M. *J. Phys. Chem.* **1995**, *99*, 4842.

(50) Madison, V.; Kopple, K. D. *J. Am. Chem. Soc.* **1980**, *102*, 4855.

(51) Baldoni, H. A.; Rodriguez, A. M.; Zamora, M. A.; Zamarbide, G. N.; Enriz, R. D.; Farkas, O.; Csaszar, P.; Torday, L. L.; Sosa, C. P.; Jakli, I.; Perzel, A.; Papp, J. G.; Hollosi, M.; Csizmadia, I. G. *J. Mol. Struct.* **1999**, *465*, 79.

(52) Hamm, P.; Lim, M.; DeGrado, W. F.; Hochstrasser, R. M. *Proc. Natl. Acad. Sci. U.S.A.* **1999**, *96*, 2036.

(53) Hamm, P.; Hochstrasser, R. M. In *Ultrafast Infrared and Raman Spectroscopy*; Fayer, M. D., Ed.; Marcel Dekker Inc.: New York, 2000; p 273.

(54) Marsh, D.; Muller, M. *Biophys. J.* **2000**, *78*, 2499.

(55) Fasman, G. D. *Poly-α-amino Acids*; Marcel Dekker: New York, 1967.

(56) Creighton, T. E. *Proteins*; W. H. Freeman & Co.: New York, 1983.

(57) Ramachandran, G. N. *Biochim. Biophys. Acta* **1974**, *359*, 298.

(58) Bohm, H.-J.; Brode, S. *J. Am. Chem. Soc.* **1991**, *113*, 7129.

(59) Frey, R. F.; Coffin, J.; Newton, S. Q.; Ramek, M.; Cheng, V. K. W.; Momany, F. A.; Schafer, L. *J. Am. Chem. Soc.* **1992**, *114*, 5369.

(60) Grubbs, W. T.; Dougherty, T. P.; Heilweil, E. J. *J. Phys. Chem.* **1995**, *99*, 10716.

(61) Laenen, R.; Simeonidis, K.; Laubereau, A. *J. Phys. Chem. B* **2002**, *106*, 408.

(62) Ambroseo, J. R.; Hochstrasser, R. M. *J. Chem. Phys.* **1988**, *89*, 5956.

(63) Oxtoby, D. W. *Adv. Chem. Phys.* **1979**, *40*, 1.